

## Controlled Modulation of Conductance in Silicon Devices by Molecular Monolayers

Tao He,<sup>†</sup> Jianli He,<sup>†</sup> Meng Lu,<sup>†</sup> Bo Chen,<sup>†</sup> Harry Pang,<sup>†</sup> William F. Reus,<sup>†</sup> Whitney M. Nolte,<sup>†</sup> David P. Nackashi,<sup>‡</sup> Paul D. Franzon,<sup>‡</sup> and James M. Tour<sup>\*†</sup>

Contribution from the Departments of Chemistry, Computer Science, Mechanical Engineering and Materials Science, and the Smalley Institute for Nanoscale Science and Technology, Rice University, Houston, Texas 77005, and Department of Electrical and Computer Engineering, North Carolina State University, Raleigh, North Carolina 27695

Received May 22, 2006; E-mail: tour@rice.edu

**Abstract:** We have controllably modulated the drain current ( $I_D$ ) and threshold voltage ( $V_T$ ) in pseudo metal-oxide-semiconductor field-effect transistors (MOSFETs) by grafting a monolayer of molecules atop oxide-free H-passivated silicon surfaces. An electronically controlled series of molecules, from strong  $\pi$ -electron donors to strong  $\pi$ -electron acceptors, was covalently attached onto the channel region of the transistors. The device conductance was thus systematically tuned in accordance with the electron-donating ability of the grafted molecules, which is attributed to the charge transfer between the device channel and the molecules. This surface grafting protocol might serve as a useful method for controlling electronic characteristics in small silicon devices at future technology nodes.

### Introduction

Although a number of alternatives to silicon-based materials have been proposed,<sup>1–3</sup> silicon remains the stalwart of the electronics industry. Generally, the behavior of silicon is controlled by changing the composition of the active region by impurity doping,<sup>4</sup> while changing the surface (interface) states is also possible.<sup>5–8</sup> As scaling to the sub-20-nm-size region is pursued, routine impurity doping becomes problematic due to its resultant uncertainty of distribution.<sup>9,10</sup> Provided back-end processing of future devices could be held to temperatures that are molecularly permissive (300–350 °C)<sup>11</sup> and taking advantage of the dramatic increase in the surface-area-to-volume ratios of small devices, it is attractive to seek controllable modulation of device performance through surface modifications.

Several techniques have been used to covalently attach molecules directly onto silicon surfaces.<sup>12–15</sup> The Si–C bond formed using these methods is both thermodynamically and kinetically stable due to its high bond strength (3.5 eV) and low polarity.<sup>15,16</sup> The majority of research in this area has focused on the grafting methods or the influence on the surface (or interface) properties of bulk semiconductors. Related work is in the use of semiconductor devices as sensors, specifically the chemically sensitive field-effect transistors (CHEMFETs)<sup>17–20</sup> and the molecularly controlled semiconductor resistor based on transistors.<sup>21–23</sup> In these devices, however, the chemicals or molecules are usually attached on the gate metal and/or insulator layer of a field-effect transistor (FET), between source and drain of an ungated FET, or on the surface metal of Schottky diodes. So far, little research has been conducted showing controlled

<sup>†</sup> Rice University.

<sup>‡</sup> North Carolina State University.

- (1) Tour, J. M. *Molecular Electronics: Commercial Insights, Chemistry, Devices, Architecture and Programming*; World Scientific: River Edge, NJ, 2003.
- (2) Seminario, J. M.; Araujo, R. A.; Yan, L. *J. Phys. Chem. B* **2004**, *108*, 6915–6918.
- (3) Reed, M. A.; Lee, T. *Molecular Nanoelectronics*; American Scientific Publishers: Stevenson Ranch, 2003.
- (4) Sze, S. M. *Semiconductor Devices: Physics and Technology*, 2nd ed.; Wiley: New York, 2001.
- (5) Ashkenasy, G.; Cahen, D.; Cohen, R.; Shanzer, A.; Vilan, A. *Acc. Chem. Res.* **2002**, *35*, 121–128.
- (6) Zhang, P.; Tevaarwerk, E.; Park, B.; Savage, D. E.; Celler, G. K.; Knezevic, L.; Evans, P. G.; Eriksson, M. A.; Lagally, M. G. *Nature (London)* **2006**, *439*, 703–706.
- (7) Boland, J. J. *Nature (London)* **2006**, *439*, 671–672.
- (8) Yang, J.; de la Garza, L.; Thornton, T. J.; Kozicki, M.; Gust, D. *J. Vac. Sci. Technol., B* **2002**, *20*, 1706–1709.
- (9) Shinada, T.; Okamoto, S.; Kobayashi, T.; Ohdomari, I. *Nature (London)* **2005**, *437*, 1128–1131.
- (10) Roy, S.; Asenov, A. *Science* **2005**, *309*, 388–390.
- (11) Liu, Z. M.; Yasserli, A. A.; Lindsey, J. S.; Bocian, D. F. *Science* **2003**, *302*, 1543–1545.

(12) Ulman, A. *Chem. Rev.* **1996**, *96*, 1533–1554.

(13) Stewart, M. P.; Maya, F.; Kosynkin, D. V.; Dirk, S. M.; Stapleton, J. J.; McGuiness, C. L.; Allara, D. L.; Tour, J. M. *J. Am. Chem. Soc.* **2004**, *126*, 370–378.

(14) Hamers R. J.; Coulter, S. K.; Ellison, M. D.; Hovis, J. S.; Padowitz, D. F.; Schwartz, M. P.; Greenlief, C. M.; Russell, J. N., Jr. *Acc. Chem. Res.* **2000**, *33*, 617–624.

(15) Buriak, J. M. *Chem. Rev.* **2002**, *102*, 1271–1308.

(16) Brook, M. A. *Silicon in Organic, Organometallic, and Polymer Chemistry*; Wiley: New York, 2000.

(17) Katz, H. E. *Electroanalysis* **2004**, *16*, 1837–1842.

(18) Nikolaides, M. G.; Rauschenbach, S.; Bausch, A. R. *J. Appl. Phys.* **2004**, *95*, 3811–3815.

(19) Janata, J. *Electroanalysis* **2004**, *16*, 1831–1835.

(20) Maruccio G.; Visconti, P.; Biasco, A.; Bramanti, A.; Torre, A. D.; Pompa, P. P.; Frascerra, V.; Arima, V.; D'Amone, E.; Cingolani, R.; Rinaldi R. *Electroanalysis* **2004**, *16*, 1853–1862.

(21) Cahen, D.; Gartsman, K.; Kadyshkevitch, A.; Naaman, R.; Shanzer, A. Hybrid Organic–Inorganic Semiconductor Structures and Sensors Based Thereon. U.S. Patent 6433356, 2002.

(22) Bartic, C.; Campitelli, A.; Borghs, S. *Appl. Phys. Lett.* **2003**, *82*, 475–477.

(23) Fritz, J.; Cooper, E. B.; Gaudet, S.; Sorger, P. K.; Manalis, S. R. *Proc. Natl. Acad. Sci. U.S.A.* **2002**, *99*, 14142–14146.

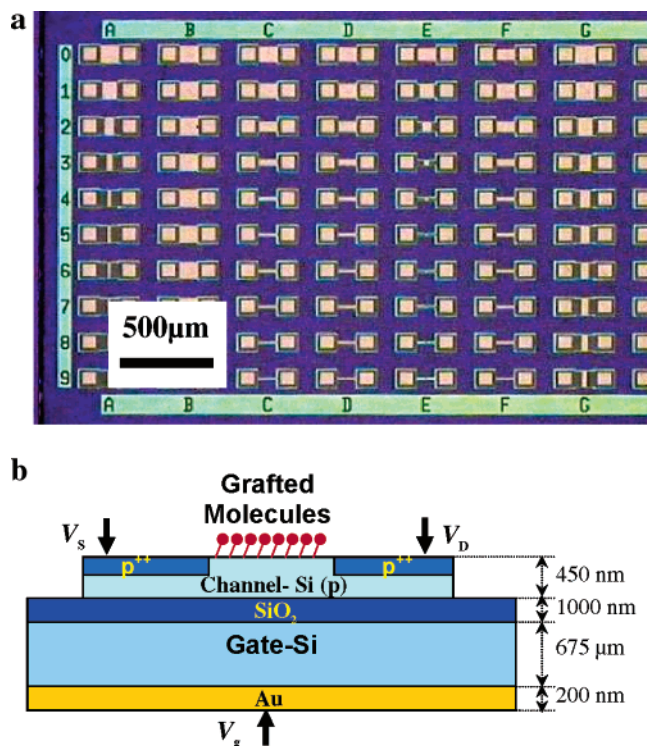


**Figure 1.** (a) An optical micrograph of some devices on one chip. Boxed regions indicate the source and drain, between which sits the channel. The data shown in this contribution were collected with Row 0, for which both the length and the width of the channel are  $100\ \mu\text{m}$  and the active area for molecular grafting is  $110 \times 110\ \mu\text{m}^2$ . (b) Schematic side-view representation (not to scale) of the device. The molecules were grafted between source and drain electrodes.  $V_s$ ,  $V_D$ , and  $V_g$  refer to the bias applied on the source, drain, and gate, respectively.

modulation of semiconductor devices by grafting molecular layers onto oxide-free active device areas, and particularly via silicon– $\text{sp}^2$ -hybridized-carbon bonds. Because there is no intervening oxide between the  $\pi$ -rich molecules and the silicon, sequentially tuned molecular-structure changes can predictably regulate the device performances over a wide range. Furthermore, gating a FET can increase the sensitivity of sensors to adsorbed chemicals.<sup>21</sup> In this contribution, an electronically controlled series of molecules, from strong  $\pi$ -electron donors to strong  $\pi$ -electron acceptors, were prepared and systematically covalently attached as molecular monolayers onto the channel region of pseudo-MOSFETs (back gated), and the device modulation was studied.

## Experimental Section

**Device Fabrication.** The pseudo-MOSFET devices were fabricated using a silicon-on insulator (SOI) wafer (Figure 1). The handle wafer was p-Si (boron doped,  $\langle 100 \rangle$ ,  $14\text{--}22\ \Omega\ \text{cm}$ ,  $675\ \mu\text{m}$  thick). The device layer was the nearly intrinsic p-Si (boron doped,  $\langle 100 \rangle$ ,  $>2000\ \Omega\ \text{cm}$ ,  $450\ \text{nm}$  thick). The BOX thickness was  $1000\ \text{nm}$ . The source and drain electrodes ( $80 \times 80\ \mu\text{m}^2$ ) were highly doped with boron at a level of about  $10^{20}\ \text{cm}^{-3}$  ( $\sim 10^{-3}\ \Omega\ \text{cm}$ ) and about  $130\ \text{nm}$  deep to get an ohmic contact. Thus, the isolated devices had  $\text{p}^{++}$  junctions. To avoid destroying the grafted molecules and interfering with their influence, we used this simple back-gating design instead of a more complicated and potentially damaging top-gate fabrication or a complicated and less robust air bridge gate design. The back contact of the structure was achieved by sputter-coating a  $200\ \text{nm}$  Au layer.

**Molecular Grafting.** Compounds **1**, **2**, and **3** were synthesized according to literature methods.<sup>24–26</sup> The synthesis of **4** is given in the

Supporting Information. The molecules **1–4** were directly grafted onto the active area in the channel region of the device using the method reported previously.<sup>13</sup> Before the molecular grafting, the devices were etched in an Ar purged buffered oxide etch (BOE, J. T. Baker, 10:1, CMOS grade) for 5 min to remove the oxide layer and form the H-passivated silicon surface. The grafting process was carried out by exposing the freshly etched samples to a  $0.5\ \text{mM}$  solution of the diazonium salt (**1–4**) in anhydrous acetonitrile ( $\text{CH}_3\text{CN}$ ) in the dark under an inert atmosphere. The grafting time depends on the molecule that was used and that was carefully calibrated. Before the grafting of molecules (**1–4**) onto the channel, we first studied the grafting protocol on a p-Si wafer (with the orientation of both  $\langle 100 \rangle$  and  $\langle 111 \rangle$ ) so as to ensure that a molecular monolayer (not a multilayer) was being formed (see Supporting Information). The grafting time was 5 h for compound **1**, 45 min for **2** and **3**, and 2 h for **4**. Molecular layer thicknesses were monitored using a single wavelength ( $632.8\ \text{nm}$  laser) Gaertner Stokes ellipsometer with an incident angle of  $70^\circ$ . X-ray photoelectron spectroscopy (XPS, PHI 5700 XPS/ESCA system) was used to ensure the molecules were directly grafted on the silicon surface. The ellipsometric and XPS results are given in the Supporting Information. After the molecular grafting, the samples were rinsed thoroughly with  $\text{CH}_3\text{CN}$  to remove the residual diazonium salt and the physisorbed materials, and then dried with an  $\text{N}_2$  flow.

**Device Testing.** The samples were tested with a probe station (Desert Cryogenics TT-prober system) under a vacuum  $<5 \times 10^{-6}$  Torr. The metal tips (ZN50R-25-BeCu or ZN50R-25-W, Desert Cryogenics) were softly probed directly onto the source/drain contacts using micron manipulators. The DC  $I(V)$  data were collected by using a semiconductor parameter analyzer (Agilent 4155C). First, all of the devices were tested immediately after the BOE etching and before the molecular grafting. To get a freshly cleaned surface for molecular grafting, the devices were then subjected to a second short etching with BOE ( $30\text{--}60\ \text{s}$ ) and were transferred into the glovebox for grafting. A second DC  $I(V)$  measurement was done after the grafting was completed. Devices with no molecules (H-passivated surface) were prepared and tested as the control samples. To study the influences from the second etching on the device performance, the control samples experienced the same treatment history as the devices under test, but without the molecular attachment, and the DC  $I(V)$  measurements were carried out after each BOE etching. Both molecular grafting and testing were done at room temperature.

## Results and Discussion

Although not the optimal design for large-scale fabrication, the pseudo-MOSFET serves as a proof-of-concept device for performance modulation by monolayer molecular grafting, obviating more rigorous designs for grafting within top-gated configurations. Note the pseudo-MOSFET structure can produce pure MOSFET-like characteristics,<sup>27</sup> which is confirmed by our experimental results. In a pseudo-MOSFET, the bulk p-Si substrate (handle) acts as a gate terminal and is biased ( $V_g$ ), through the Au back contact, to induce a conduction channel at the upper interface of the buried oxide (BOX). This BOX is used as a gate dielectric layer. As in our case, an accumulation channel (p-channel) was activated when both the gate ( $V_g > V_T$ ) and the drain were negatively biased. Because the transistor body is the nearly intrinsic p-Si layer ( $>2000\ \Omega\ \text{cm}$  and  $450\ \text{nm}$  thick), the channel is assumed to be completely accumulated.

- (24) Becker, H. G. O.; Grossmann, K. J. *Prakt. Chem.* **1990**, *332*, 241–250.  
 (25) Milz, H.; Schladetsch, H. J. *Monodiazotization of Aromatic Diamines*; Ger. Offen., 1977; 15 pp.  
 (26) Dai, M. J.; Liang, B.; Wang, C. H.; Chen, J. H.; Yang, Z. *Org. Lett.* **2004**, *6*, 221–224.  
 (27) Cristoloveanu, S.; Williams, S. *IEEE Electron Device Lett.* **1992**, *13*, 102–104.

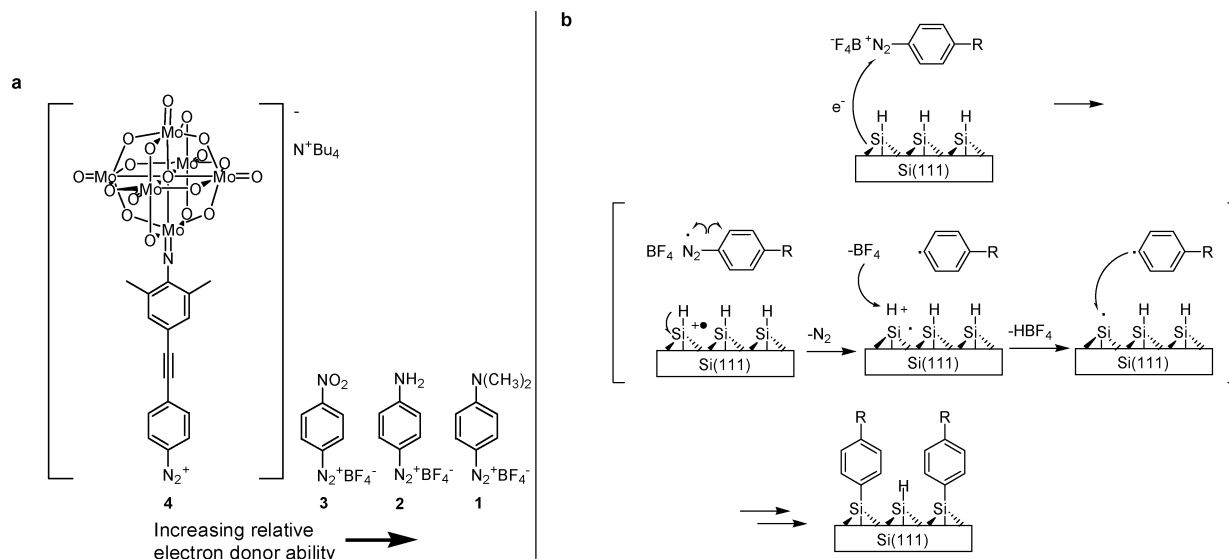


**Figure 2.** (a) Molecular structures used for grafting atop the pseudo-MOSFET channel. Structures of the starting molecules **1–4** used in the present contribution where **1** is the most electron-rich system due to the dimethylamino substituent, **2** is slightly lower in its electron donation capability, followed by **3**, and then finally **4** bears an extremely electropositive polymolybdate. (b) The mechanism of the reaction of H-passivated Si with aryldiazonium salts is illustrated.<sup>13</sup> In this case, the R-group represents the *para*-moiety on the grafted aryl ring.

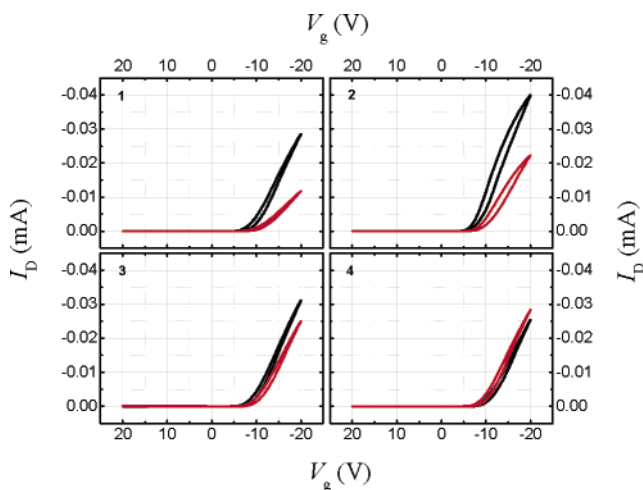


**Figure 3.** Transfer characteristics of the devices under test before (black) and after (red) the grafting of different molecular monolayers. The numbers (1, 2, 3, and 4) in the illustrations correspond to compounds **1–4**, respectively. Data shown here were collected under  $-5$  V of  $V_D$  and are the average value for 14 devices from Row 0 on one chip, as described in Figure 1a, and they are characteristic of the hysteresis observed in all of the devices. The gate bias was scanned first from  $+20$  to  $-20$  V (forward) and then back from  $-20$  to  $+20$  V.

The source and drain areas were highly doped ( $10^{20}$   $\text{cm}^{-3}$ ) to ensure ohmic contact when metal tips were brought to probe the source and drain electrodes. Because the doping levels of the junctions are much greater than that of the channel, the influences of the source and drain parasitic series resistances were negligible. The molecules (Figure 2a) were grafted in the channel region between the drain and source electrodes. The diazonium portion of the molecule was lost, resulting in a direct aryl–silicon bond (Figure 2b), as we have described previously.<sup>13</sup>

Figure 3 shows the typical transfer characteristics of the devices under test before and after the grafting of molecular monolayers. It is assumed there are no short- or narrow-channel effects because both the length and the width of the device channel used here were  $100$   $\mu\text{m}$ . For compounds **1–3**, the drain current under the same gate bias decreased after the molecular

grafting. The amplitude of this decrease is in the order of  $1 > 2 > 3$ . Yet  $I_D$  increased slightly after the grafting of **4**. The hysteresis observed in the  $I_D$ – $V_g$  curves are very similar in amplitude and shape before and after the molecular attachment (Figure 3). Therefore, these hysteretic effects are caused by the device itself, not by the molecular grafting.

$V_T$  can be extracted based on the measurement of  $I_D$ , which represents the onset of significant drain current and is a fundamental parameter for MOSFET characterization and modeling. The  $V_T$  values shown here were determined from the  $V_g$  axis intercept of the  $I_{D,\text{Sat}}^{0.5}$ – $V_g$  characteristics linearly extrapolated,<sup>28–30</sup> as shown in Figure 4a (also see Supporting Information). Figure 4b shows the representative change in  $V_T$  ( $\Delta V_T$ ) of the devices under test before and after the grafting of molecular monolayers. It is seen from Figure 4b that the  $V_T$  became more negative (usually about  $1$ – $2$  V) after grafting **1**, **2**, and **3**, while it became less negative for **4**, relative to the control, which was the Si–H surface before molecular grafting. Although there are slight differences between the values of  $\Delta V_T$  when  $V_T$  was extracted from the forward and back scans (Figure 4b) due to the inherent hysteretic nature of the devices themselves (Figure 3), the same trend in the change of  $V_T$  was observed for the control. The control samples experienced the same treatment history as the devices under test, but had no molecules grafted on them, only the hydrogen passivation remained. For control samples, the  $V_T$  changed slightly (typically  $\leq 0.3$  V) from the first to the second etching. This supports our assertion that the  $V_T$  change in the devices under test is not caused by the etching but by the molecular grafting on the channel region, which tracks directly with the electron donor ability of the molecules.

The changes in  $V_T$  after the monolayer molecular grafting are consistent with those in  $I_D$ . Attaching compounds **1–3** led

- (28) Terada, K.; Nishiyama, K.; Hatanaka, K. *Solid-State Electron.* **2001**, *45*, 35–40.  
 (29) Schroder, D. K. *Semiconductor Material and Device Characterization*, 3rd ed.; Wiley: Hoboken, 2006.  
 (30) Ortiz-Conde, A.; Sánchez, F. J. G.; Liou, J. J.; Cerdeira, A.; Estrada, M.; Yue, Y. *Microelectron. Reliab.* **2002**, *42*, 583–596.

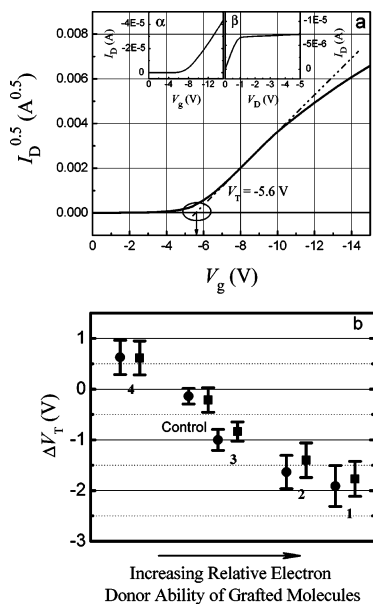


**Figure 4.** Electrical output results of the pseudo-MOSFET devices. (a) Extrapolation method for  $V_T$  used on the measured  $I_{D,sat}^{0.5}-V_g$  characteristics.  $V_T$  was extracted at its maximum slope point. Inset  $\alpha$  displays the typical transfer characteristics of the devices under test with an applied drain-source bias ( $V_D$ ) of  $-5$  V. Such a  $V_D$  was chosen for the  $V_T$  extraction according to inset  $\beta$ , the typical output characteristics of the devices under test at  $V_g > V_T$ , to ensure the device operation was in the saturation region (Supporting Information). (b) Representative  $\Delta V_T (= V_{T(\text{with molecules})} - V_{T(\text{without molecules})})$  of the devices under test extracted from both the forward (●) and the back (■) scans after the grafting of different molecular monolayers (**1–4**), as well as on the control samples. Data shown here are the average value for 14 devices identical to those in Figure 3. The vertical bars indicate standard deviations for each of the 14 devices tested.

to a more negative  $V_T$  and less  $I_D$ , while attaching **4** resulted in a less negative  $V_T$  and larger  $I_D$ . Therefore, the channel conductances were reduced by grafting molecular monolayers of **1–3**, and they were increased by **4**, scaling directly with the relative electron-donating ability of the molecules.

During the grafting process, hydrogen atoms on the H-passivated surface were replaced by the molecules and new aryl–silicon bonds were formed (Figure 2b). Some H-passivated sites remain due to steric constraints on the grafting, as seen by surface IR analysis.<sup>13</sup> Nevertheless, the resultant monolayers are dense enough to provide significant surface-passivation against electrochemical faradaic charging, and they are even stable to short buffered oxide or KOH etching.<sup>13</sup> Based on this packing of molecules and on the observed electrical results, the mechanisms are discussed below.

A molecular monolayer with a positive dipole (here, the sign of the molecular dipole is arbitrarily chosen to be positive if its negative pole points away from the surface after grafting) is induced by compounds **3** and **4**, while a negative dipole is induced for **1** and **2**. Although it is realized that the resultant dipole layer on the surface can create an electrostatic potential that would produce effects similar to those induced by a gate bias in a standard MOSFET,<sup>31</sup> the model that the molecular monolayer acts as a top gate is not considered in our case because it cannot explain why **1** and **2** have the same effects as **3**, or why **3** and **4** (with the same dipole polarity) exhibit opposite effects. Furthermore, it seems unreasonable to simply add such a local field to the external field.

The fact that grafting molecular monolayers onto the channel region can change its conductance is mildly analogous, from a

charge perspective, to that of the impurity doping. Considering an accumulation channel (p-channel) was formed in our pseudo-MOSFETs, the acceptor-like monolayer (more potent than the hydrogen atom of the H-passivated control) would decrease the  $V_T$  of the pseudo-MOSFET and the donors would increase the  $V_T$ . Following this suggestion, the data imply that p-Si gained negative charges when modified by compounds **1–3**, while it gave up negative charges in the case of **4**. A simple calculation (Supporting Information) implies that a 1 V change in  $V_T$  corresponds to the transfer of about 0.002 elementary charges per grafted molecule, a value consistent with electrostatic effects of organic molecules on neighboring bodies.<sup>32</sup> Such a charge-transfer process is dependent on several factors. During the molecular grafting, Si–C bonds were formed between the aryl ring and lightly boron-doped silicon. The  $\pi$ -electron cloud from the aryl system is in close interaction with the silicon surface, and thus the different molecular effects may originate from the functional group of the attached molecules. Because the functional groups of **1** ( $-\text{N}(\text{CH}_3)_2$ ) and **2** ( $-\text{NH}_2$ ) are donors, the density of this  $\pi$ -electron cloud is higher than that of **3** ( $-\text{NO}_2$ ), an acceptor, and **4** (polymolybdate cluster), a potent acceptor.<sup>33–36</sup> So it is reasonable that, relative to the H-passivated surface, **1** and **2** act as the electron donor while **4** acts as the acceptor. This agrees with our experimental results. However, it cannot explain the location of **3** in Figure 4b. Note this designation of acceptor for the  $-\text{NO}_2$  moiety is relative to a hydrogen atom at the 4-position of a phenyl ring, and here we are comparing a 4-nitrophenylene ( $4\text{-C}_6\text{H}_4\text{-NO}_2$ ) as assembled in **3** to simply a hydrogen atom directly bonded to the silicon surface in the H-passivated control. The 4-nitrophenylene, with its  $\pi$ -electron cloud from the aryl system in close interaction with the silicon surface, may still be acting as an electron donor relative to the H-passivated surface. It is not until we go to a very strong electron-withdrawing group as in the polymolybdate cluster **4** that we are able to shift the electron-withdrawing effect sufficiently past that of the control surface. Indeed, nitrobenzene has a more negative reduction potential than that of the aryl polymolybdate cluster,<sup>33–35</sup> confirming **4** as the most potent acceptor in the series. This also explains why the change in  $V_T$  was observed in the series **1** > **2** > **3** > **4**.

In addition, replacing the hydrogen atoms on the H-passivated surface by molecules may generate new surface states. It has been reported that surface or interface bands can modulate the thermal excitation of bulk carriers in thin silicon layers.<sup>6</sup> Because a dipole layer is present on the surface and considering the dipole–dipole interactions, additional charge redistribution at the surface or interface is induced.<sup>25,37–39</sup> This can also affect the charge-transfer process. The dipole moment may be different

- (31) Cahen, D.; Naaman, R.; Vager, Z. *Adv. Funct. Mater.* **2005**, *15*, 1571–1578.
- (32) Seminario, J. M.; Yan, L.; Ma, Y. *Proc. IEEE* **2005**, *10*, 1753–1764.
- (33) Lu, M.; Xie, B.; Kang, J.; Chen, F.; Yang, Y.; Peng, Z. *Chem. Mater.* **2005**, *17*, 402–408.
- (34) Kang, J.; Nelson, J. A.; Lu, M.; Xie, B.; Peng, Z.; Powell, D. R. *Inorg. Chem.* **2004**, *43*, 6408–6413.
- (35) Donkers, R. L.; Workentin, M. S. *Chem.-Eur. J.* **2001**, *7*, 4012–4020.
- (36) Smith, M. B.; March, J. *Advanced Organic Chemistry: Reactions, Mechanisms, and Structure*, 5th ed.; Wiley: New York, 2001; p 370.
- (37) Hutchison, G. R.; Ratner, M. A.; Marks, T. J.; Naaman, R. J. *Phys. Chem. B* **2001**, *105*, 2881–2884.
- (38) Selzer, Y.; Cai, L. T.; Cabassi, M. A.; Yao, Y. X.; Tour, J. M.; Mayer, T. S.; Allara, D. L. *Nano Lett.* **2005**, *5*, 61–65.
- (39) Salomon, A.; Boecking, T.; Chan, C. K.; Amy, F.; Girshevitz, O.; Cahen, D.; Kahn, A. *Phys. Rev. Lett.* **2005**, *95*, 266807.

from molecule to molecule. The tilt angle and coverage or density of the grafted molecules might also be quite different between the molecular groups **1–3** (all being about the same molecular size) and molecule **4** (being relatively large and more difficult to pack). All of this leads to unique charge redistributions and the resulting molecular effects that depend on the relative structures of the grafted molecules and their resultant monolayers. Hence, the charge-transfer process is closely related to the alignment of the molecular and surface energy levels in the devices.<sup>2,40–42</sup>

### Summary

In this contribution, we demonstrated that, by grafting a monolayer of molecules atop oxide-free H-passivated silicon surfaces (channel region), the drain current and threshold voltage in pseudo MOSFETs can be systematically modulated over a wide electronic range in accordance with the electron-donating

ability of the grafted molecules. This effect is ascribed to the charge transfer between the device channel and the molecules. This could serve as an excellent method to controllably tune electronic performance in nanoscale devices (large surface-area-to-volume ratios) through surface grafting where consistent impurity doping becomes hard to achieve due to doping profile inhomogeneities between devices.

**Acknowledgment.** This work was supported by the Defense Advanced Research Projects Agency through the Air Force Office of Scientific Research.

**Supporting Information Available:** Detailed information on the experimental methods, the XPS and ellipsometric characterization of silicon grafted with molecules, extraction of threshold voltages, output characteristics of the devices, and the calculation of charge transfer between the molecules and the device layer. This material is available free of charge via the Internet at <http://pubs.acs.org>.

- (40) Iozzi, M. F.; Cossi, M. *J. Phys. Chem. B* **2005**, *109*, 15383–15390.  
(41) Natan, A.; Zidon, Y.; Shapira, Y.; Kronik, L. *Phys. Rev. B* **2006**, *73*, 193310.  
(42) Cohen, R.; Kronik, L.; Shanzer, A.; Cahen, D.; Liu, A.; Rosenwaks, Y.; Lorenz, J. K.; Ellis, A. B. *J. Am. Chem. Soc.* **1999**, *121*, 10545–10553.

JA063571L